A Letters Journal Exploring
the Frontiers of Physics

OFFPRINT

Quantum chaotic scattering in graphene systems

R. Yang, L. Huang, Y.-C. Lai and C. Grebogi

EPL, **94** (2011) 40004

A Letters Journal Exploring the Frontiers of Physics

May 2011

EPL, **94** (2011) 40004 www.epljournal.org
doi: 10.1209/0295-5075/94/40004

Quantum chaotic scattering in graphene systems

Rui Yang[1], Liang Huang[1,2], Ying-Cheng Lai[1,3,4] and Celso Grebogi[4]

[1] *School of Electrical, Computer and Energy Engineering, Arizona State University - Tempe, AZ 85287, USA*
[2] *Institute of Computational Physics and Complex Systems, and Key Laboratory for Magnetism and Magnetic Materials of MOE, Lanzhou University - Lanzhou, Gansu 730000, China*
[3] *Department of Physics, Arizona State University - Tempe, AZ 85287, USA*
[4] *Institute for Complex Systems and Mathematical Biology, School of Natural and Computing Sciences, King's College, University of Aberdeen - Aberdeen, UK, EU*

received 5 December 2010; accepted in final form 8 April 2011
published online 11 May 2011

PACS 05.45.Mt – Quantum chaos; semiclassical methods
PACS 72.80.Vp – Electronic transport in graphene
PACS 73.23.-b – Electronic transport in mesoscopic systems

Abstract – We investigate the transport fluctuations in both non-relativistic quantum dots and graphene quantum dots with both hyperbolic and nonhyperbolic chaotic scattering dynamics in the classical limit. We find that nonhyperbolic dots generate sharper resonances than those in the hyperbolic case. Strikingly, for the graphene dots, the resonances tend to be much sharper. This means that transmission or conductance fluctuations are characteristically greatly enhanced in relativistic as compared to non-relativistic quantum systems.

In the last three decades, quantum chaos, an interdisciplinary field focusing on the quantum manifestations of classical chaos, has received a great deal of attention [1]. In fact, the quantization of chaotic Hamiltonian systems and the ensuing quantum signatures of classical chaos are fundamental procedure and process, respectively, in physics, having direct applications in condensed matter physics, atomic physics, nuclear physics, optics, and acoustics. However, most existing works on quantum chaos are concerned with non-relativistic quantum-mechanical systems described by the Schrödinger equation. Since the quasi-particles of graphene are chiral, massless Dirac fermions [2,3], the fundamental issue of *relativistic* quantum manifestations of chaos in graphene systems has attracted a great deal of recent attention. Topics that have been studied include level-spacing statistics, transition from regular to chaotic dynamics, relativistic quantum scars, and weak localization, etc. [4,5]. In this letter, we study the fundamental problem of *relativistic* quantum scattering using graphene chaotic billiards and compare the results with those from non-relativistic quantum-dot systems.

In open Hamiltonian systems, there are two kinds of dynamically relevant chaotic scattering processes: hyperbolic and nonhyperbolic. Both are highly relevant experimentally. In hyperbolic scattering, all the periodic orbits are unstable and the particle decay law is exponential. As a result, the magnitude squared of the autocorrelation function of the quantum S-matrix elements is Lorentzian, where the classical escape rate determines its half-width [6]. The Lorentzian form has been observed experimentally [7]. For nonhyperbolic chaotic scattering, there are non-attracting chaotic sets coexisting with Kolmogorov-Arnold-Moser (KAM) tori in the phase space [8], leading to an algebraic particle decay law. In this case, the fine-scale semiclassical quantum fluctuations of the S-matrix elements with energy difference are *enhanced* as compared to the hyperbolic case [8]. We note that for a classically integrable billiard system, Bardarson *et al.* [9] solved the Dirac equation and observed sharp resonances in the conductance-fluctuation pattern.

To uncover the relativistic quantum manifestations of chaotic scattering, in this letter we investigate the electronic transport properties in open graphene quantum dots (GQDs) with both hyperbolic and nonhyperbolic scattering dynamics in the classical limit. We compare the GQD analysis with the one we carry out for non-relativistic quantum dot (NRQD) systems. A striking finding is that GQDs generally have sharper conductance fluctuations than NRQDs [10]. Moreover, GQDs tend to stabilize unstable periodic orbits, which support the hyperbolic scattering. As a result, even in the hyperbolic GQDs, pronounced quantum pointer states [14,15] exist. The resonances associated with the transmission are characterized by the Fano profiles with the width given by the imaginary part of the eigenenergies of the dot Hamiltonian, where the effects of the leads are theoretically described by the self-energies. Our findings not only provide fundamental insights into relativistic quantum chaotic scattering, but also are important for graphene-based device applications.

To systematically investigate the quantum scattering dynamics in open graphene quantum dots, it is desirable to focus on a class of dot systems that can generate both hyperbolic and nonhyperbolic chaotic scattering dynamics. We choose the class of cosine billiards [11], which is defined by two hard walls at $y = 0$ and $y(x) = W + (M/2)[1 - \cos(2\pi x/L)]$, respectively, for $0 \leqslant x \leqslant L$, with two semi-infinite leads of width W attached to the left and right openings of the billiard. By adjusting the ratios W/L and M/L, the stabilities of the classical periodic orbits can be changed, allowing the transition from nonhyperbolic to hyperbolic chaotic scattering. For example, for $W/L = 0.18$ and $M/L = 0.11$, there is nonhyperbolic scattering but for $W/L = 0.36$ and $M/L = 0.22$, the scattering dynamics is hyperbolic [11]. We use the tight-binding approach and the Landauer-Büttiker formalism in combination with the non-equilibrium Green's function method to calculate the conductance/transmission and the local density of states (LDS) [16,17]. All energies are given in units of the hopping energy t.

We evaluate the transmission fluctuations for the four combinations of quantum dots and classical scattering dynamics: NRQD/hyperbolic, NRQD/nonhyperbolic, GQD/hyperbolic, and GQD/nonhyperbolic. All the quantum dots have the same maximum number of propagating modes: $N_{\mathrm{mode}} = 24$, and GQDs have zigzag boundaries terminated in the horizontal direction. Typical patterns of the transmission fluctuations are shown in fig. 1, where the energy ranges are the same for different cases. The results for NRQDs (fig. 1(a)) are consistent with those from previous works, *i.e.*, the one with nonhyperbolic chaotic scattering in the classical limit exhibits sharper fluctuations, while if the classical scattering dynamics is hyperbolic, the transmission varies much more smoothly with the energy [11]. Similar behaviors have been observed for GQDs, as shown in fig. 1(b), which is consistent with the results in ref. [9]. However, comparing figs. 1(b) and (a), we see apparently enhanced fluctuations in the graphene case, for both hyperbolic and nonhyperbolic chaotic scattering. Even in the hyperbolic case, the transmission associated with the GQD contains sharper resonances as compared with that in the NRQD. This indicates a strong localization effect [12,13] in the GQD.

To characterize the fluctuations, we compute the autocorrelation function from the transmission *vs.* energy curve after removing the smooth background variation. The results are shown in fig. 2. As expected, for the GQDs, the correlation functions decay faster than those for NRQDs,

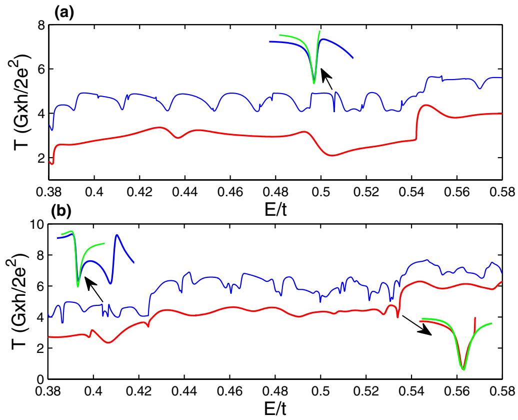

Fig. 1: (Color online) Transmission T *vs.* energy E for open (a) non-relativistic and (b) graphene quantum dot with the same maximum number of propagating modes: $N_{\mathrm{mode}} = 24$. Blue/thin (red/thick) lines are for nonhyperbolic (hyperbolic) scattering dynamics in the classical limit. Note that, to clearly distinguish these two lines in each figure, we shift the transmissions for hyperbolic ones (red/thick) down by 1. The insets show the fitting lines (green) using eq. (1). The energy values E_0/t corresponding to the three cases are (a) 0.50581, (b/left) 0.40402, and (b/right) 0.53392.

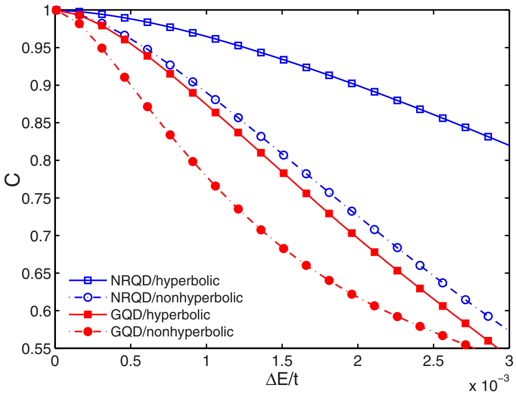

Fig. 2: (Color online) Autocorrelation C *vs.* energy difference ΔE for different quantum dots with $N_{\mathrm{mode}} = 48$.

indicating stronger fluctuations of the transmission or, equivalently, a smaller energy scale over which a large change in the transmission can occur. This is consistent with the recent result that GQDs tend to have enhanced conductance fluctuations in the presence of disorder, due to the absence of back scattering [18] or to the Andreev reflection at the graphene-superconductor interface [19].

To provide a theoretical explanation for these phenomena, we examine the Fano resonances with respect to the coupling between the eigenstates in the quantum dots and the leads. We find that the coupling is typically much weaker in the GQD than that in the NRQD for both the hyperbolic and nonhyperbolic cases. In particular, in the tight-binding paradigm, by considering the scattering region as a closed system with Hamiltonian matrix H_c, the effect of the leads can be treated using the retarded self-energy matrices, $\Sigma^R = \Sigma^R_L + \Sigma^R_R$. The matrix H_c is Hermitian with a set of real eigenenergies and eigenfunctions $\{E_{0\alpha}, \psi_{0\alpha} | \alpha = 1, \ldots, N\}$, but $\Sigma^R(E)$ is in general not Hermitian and depends on the Fermi energy E. The effective Hamiltonian matrix $H_c + \Sigma^R(E)$ thus has a set of complex eigenenergies with the eigenfunctions: $[H_c + \Sigma^R(E)]\psi_\alpha = E_\alpha \psi_\alpha$ and $\phi^T_\alpha [H_c + \Sigma^R(E)] = E^*_\alpha \phi^T_\alpha$, where $E_\alpha = E_{0\alpha} - \Delta_\alpha - i\gamma_\alpha$. The self-energy matrix Σ^R has only nonzero elements in the subblock of the boundary atoms connecting with the leads. For most of the eigenstates it can be treated as a perturbation, thus Δ_α and γ_α are generally small.

The Green's function matrix can be expanded as $G^R(E) = \sum_\beta [\psi_\beta(E)\phi_\beta(E)^\dagger]/[E - E_\beta(E)]$. For a particular eigenstate $\{E_\alpha, \psi_\alpha\}$, when E is close to E_α, G^R can be rewritten as $G^R = G^R_0(E) + G^R_1(E)$, where $G^R_0(E) = \sum_{\beta \neq \alpha} [\psi_\beta(E)\phi_\beta(E)^\dagger]/[E - E_\beta(E)]$ varies slowly since $|E - E_\beta|$ is large and $G^R_1(E) = [\psi_\alpha(E)\phi_\alpha(E)^\dagger]/[E - E_\alpha(E)]$ changes fast as E is in the vicinity of E_α. The self-energy Σ^R is a slow variable, so is the coupling matrix $\Gamma^R_{L,R} = i[\Sigma^R_{L,R} - (\Sigma^R_{L,R})^\dagger]$. Thus in the expression of the transmission $T = \mathrm{Tr}[\Gamma^R_L G^R \Gamma^R_R (G^R)^\dagger]$, only $G^R_1(E)$ is a fast variable. All the others can be treated approximately as constants and be evaluated at an arbitrary energy E_0 close to E_α. Choosing $E_0 = E_\alpha$, we get the transmission in the vicinity of E_α as $T(E) \approx T_0(E_0) + \Delta T(1 - 2q\varepsilon)/(\varepsilon^2 + 1)$, where $T_0 = \mathrm{Tr}[\Gamma^R_L G^R_0 \Gamma^R_R (G^R_0)^\dagger]$, $\Delta = T(E_0) - T_0(E_0)$, $q = \mathrm{Im}(\mathrm{Tr}[\Gamma^R_L G^R_1 \Gamma^R_R (G^R_0)^\dagger])/\Delta T$, and $\varepsilon = (E - \mathrm{Re}(E_\alpha))/\gamma_\alpha$. We thus have

$$T(E) \approx T_0(E_0) - \Delta T + \Delta T \frac{(\varepsilon - q)^2}{\varepsilon^2 + 1} + \Delta T \frac{2 - q^2}{\varepsilon^2 + 1}. \quad (1)$$

As shown in fig. 1, this formula agrees with numerical results very well, which represents a generalized Fano resonance, and is consistent with previous works on Fano resonance profiles of conductance by calculating the scattering matrix elements [13,20][1]. Thus the transmission curve has a resonance at $\mathrm{Re}(E_\alpha)$, where the width is on the order of γ_α. Since Σ^R depends on the energy E, Δ_α and γ_α are also functions of E. Thus the above picture is valid only for eigenstates whose values of $\mathrm{Re}(E_\alpha)$ are close to E [17].

The above analysis requires γ_α to be much smaller than the level spacing between the adjacent energy levels, *i.e.*, for separated and localized states. For large γ_α, the resonances are broadened and it then becomes difficult to distinguish them from the background variations. This is the reason that, for NRQDs with nonhyperbolic scattering dynamics, a similar analysis can be valid only when strong localizations on stable periodic orbits occur [13]. For GQDs, our computations have revealed sharp conductance resonances (figs. 1 and 2) for both hyperbolic and nonhyperbolic classical scattering dynamics, leading to small values of γ_α. Figure 3 shows the eigenenergies E_α in the complex plane in a proper energy range. The energy for which the self-energy matrix is evaluated is $E_0 = 0.2t$ for GQDs and $E_0 = t$ for NRQDs. In principle, the plots are only accurate for the eigenenergies where $\mathrm{Re}(E_\alpha)$ is close to E_0 but we find that, even if $\mathrm{Re}(E_\alpha)$ is far from E_0, it is still a good approximation. We have also examined larger systems with the same shapes. For a larger system, there are more points in the plots, but the distribution of the points remains the same. These results verify those in fig. 2 in that the system with smaller γ_α values decreases faster in the correlation function. From fig. 3, we see that, the four cases have the common feature that they all possess a continuous line shape about $\gamma_\alpha \sim 10^{-2}t$. These values contribute to the conductance variations on energy scales of $10^{-2}t$ to $10^{-1}t$ and hence to the smooth conductance variations in the background. For NRQDs, only the hyperbolic case has this part, but the nonhyperbolic case has relatively lower values in the range $10^{-4}t$ to $10^{-2}t$ (fig. 3(b)), which correspond to the localized states. The separation between the two parts is not sharp, due to the heterogeneous, mixed phase-space structure associated with nonhyperbolic chaotic scattering [12]. For GQDs, for both the hyperbolic and nonhyperbolic cases, the distributions of the eigenenergies contain two parts: one with and the other without localized states. For the nonhyperbolic case, the two parts are well separated and the lower part is several orders of magnitude smaller than that associated with the nonhyperbolic NRQD, as shown in fig. 3(a), indicating much sharper transmission fluctuations. Furthermore, the hyperbolic GQD also contains such a

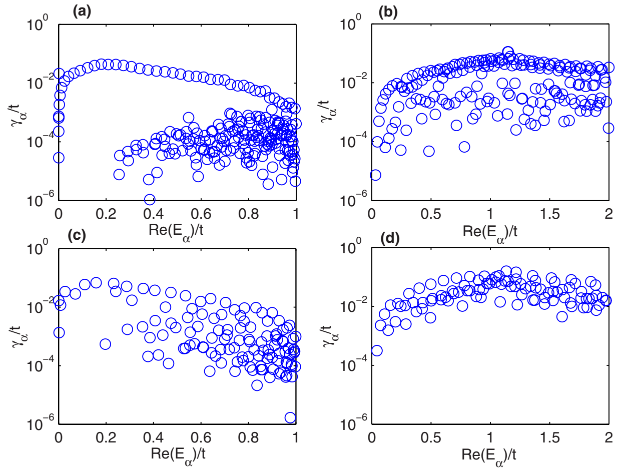

Fig. 3: (Color online) The real and imaginary part of the eigenstates E_α for (a) GQD/nonhyperbolic, (b) NRQD/nonhyperbolic, (c) GQD/hyperbolic, and (d) NRQD/hyperbolic. The energy values E_0 in (a)–(d) are 0.2, 1, 0.2 and 1, respectively.

[1] In the Fano formula, $(\varepsilon + q)^2/(\varepsilon^2 + 1)$, the quantity q usually takes on real values. However, as pointed out in ref. [20], when characterizing conductance fluctuations, q can generally be complex: $q = q' + iq''$. In this case, the Fano profile becomes $|\varepsilon + q|^2/(\varepsilon^2 + 1) = [(\varepsilon + q')^2 + q''^2]/(\varepsilon^2 + 1)$, which is the same as eq. (1) when $q'^2 + q''^2 = 2$. A similar relation was observed in a previous experimental study [21].

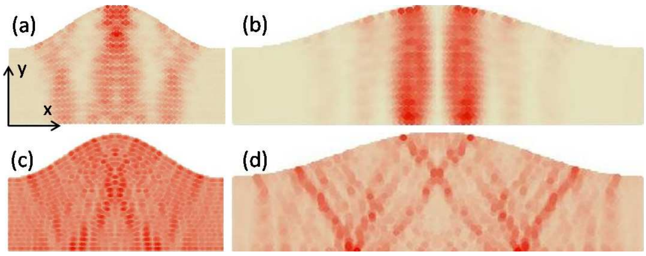

Fig. 4: (Color online) Quantum pointer states for (a) GQD/ hyperbolic, (b) GQD/nonhyperbolic, (c) NRQD/hyperbolic, and (d) NRQD/nonhyperbolic. Darker region means higher local density of states (LDS). The minimum and maximum LDS values of the patterns are (2.59×10^{-3}, 0.641), (5.84×10^{-4}, 1.39), (8.50×10^{-3}, 7.35×10^{-2}), (1.40×10^{-2}, 0.284) for (a)–(d), respectively. The color scale has been normalized for each panel for better visualization.

lower part (figs. 3(c)), providing an explanation for the observed sharp resonances in fig. 1(b).

Although the classical scattering dynamics are purely chaotic and the quantum manifestations are expected of those situations where there is no strong localization, the same quantum dot filled with graphene shows characteristically different behaviors. For example, we find that relativistic quasiparticles in graphene tend to stabilize themselves on the *classically unstable* periodic orbits. This can be demonstrated directly from the LDS patterns. Figure 4 shows a typical pattern for each of the four combinations. For nonhyperbolic NRQD and GQD, the LDS patterns are well localized, but the patterns for the GQD are much sharper than those for the NRQD. For the hyperbolic cases, again the patterns associated with the NRQD are not so sharp, as exemplified by fig. 4(c), but for the GQD, there are still many well-pronounced pointer states, as the one shown in fig. 4(a). Since a graphene billiard has two nonequivalent Dirac points and the abrupt boundary introduces coupling between them, the observed transmission fluctuations and the tendency to stabilize unstable periodic orbits can be originated from both effects: relativistic motion of the pseudo-particle in graphene and the coupling between the two Dirac points.

A key to understanding the distinct characteristics of the transmission in NRQDs and GQDs with different types of chaotic scattering in the classical limit is the relation between the LDS patterns and the width of the resonances. We have calculated the first-order approximation of γ_α. In the absence of magnetic field, H_c is real symmetric, so $\{\psi_{0\alpha}|\alpha=1,\ldots,N\}$ forms a set of orthogonal and complete basis. Generally, we have $\psi_\alpha=\psi_{0\alpha}-\delta_r\psi_{\alpha r}-i\delta_i\psi_{\alpha i}$, where δ_r and δ_i are small quantities. Substituting E_α and ψ_α back into the eigenequation $[H_c+\Sigma^R]\psi_\alpha=E_\alpha\psi_\alpha$, keeping only the first-order terms and taking into account the orthogonality of $\psi_{0\alpha}$, we have $\Delta_\alpha+i\gamma_\alpha\approx-\langle\psi_{0\alpha}|\Sigma^R|\psi_{0\alpha}\rangle$. Thus, $\gamma_\alpha=-\langle\psi_{0\alpha}|\mathrm{Im}(\Sigma^R)|\psi_{0\alpha}\rangle$. That is, the width of the transmission resonance (γ_α) is determined by the imaginary part of the self-energy and the corresponding wave function of the closed system. Since Σ^R only has nonzero elements at the boundary atoms connecting with the leads, only the values of $\psi_{0\alpha}$ on the same set of atoms contribute to γ_α. Since the wave function is normalized, localized states that assume a large value on a subset of atoms, say, atoms on a particular stable orbit, will have small values on the boundary atoms, resulting in small values of γ_α. For dispersive states where $\psi_{0\alpha}$ takes similar values on all atoms, the value on the boundary atoms are of the order of $1/\sqrt{N}$. Thus γ_α depends mainly on Σ^R. For cases of identical leads, Σ^R is the same, thus $\gamma_\alpha\sim1/N$. Nonhyperbolic QDs have about twice the number of atoms as the hyperbolic QDs, so γ_α is about half the value, which has been verified numerically. We note that the effect caused by the system size changes the results by a factor of 2, while the features of localization (the structure of the phase space, *i.e.*, whether it has KAM-tori and the ratio of the regular KAM-tori *vs.* chaotic sea) can contribute to the difference in γ_α by several orders of magnitude. Since the eigen-wavefunctions are highly correlated with the LDS patterns, the above discussion should also be valid for LDS patterns, or pointer states.

In summary, we have examined the transport fluctuations for GQDs and NRQDs that exhibit both hyperbolic and nonhyperbolic chaotic scattering in the classical limit. For each type of QDs, the one with classical nonhyperbolic scattering dynamics exhibits enhanced transmission fluctuations with sharp resonances compared to that with hyperbolic dynamics, which is consistent with previous results in quantum chaotic scattering. However, in GQDs, the fluctuations are much stronger with smaller energy scales as compared with NRQDs. By examining the width of the transmission resonances, we find a theoretical explanation for the enhanced fluctuations in GQDs: scarring of quantum states in the graphene system are more pronounced, resulting in weaker coupling with the leads as compared with NRQDs. Computation of the LDS supports this theory. From another point of view, since the width of the transmission resonance is typically smaller than the level spacing ΔE (eq. (1)), the non-constant density of states for GQDs, in contrast to a constant level spacing for NRQD, can be responsible for the sharp conductance fluctuations. In general, we expect then the transmission (or scattering-matrix elements) to exhibit characteristically enhanced fluctuations in relativistic compared to those in non-relativistic quantum mechanics.

* * *

This work was supported by AFOSR under Grant No. FA9550-09-1-0260 and by ONR under Grant No. N00014-08-1-0627. CG was supported by BBSRC under Grants No. BB-F00513X and No. BB-G010722. LH was also supported by NSFC under Grant No. 11005053.

REFERENCES

[1] See, for example, Gutzwiller M. C., *Chaos in Classical and Quantum Mechanics* (Springer, New York) 1990; Stöckmann H. J., *Quantum Chaos: An Introduction* (Cambridge University Press, Cambridge, UK) 1999; Heller E. J., *Phys. Rev. Lett.*, **53** (1984) 1515.

[2] Wallace P. R., *Phys. Rev.*, **71** (1947) 622.

[3] Castro Neto A. H., Guinea F., Peres N. M. R., Novoselov K. S. and Geim A. K., *Rev. Mod. Phys.*, **81** (2009) 109.

[4] Novoselov K. S., Geim A. K., Morozov S. V., Jiang D., Zhang Y., Dubonos S. V., Grigorieva I. V. and Firsov A. A., *Science*, **306** (2004) 666; Novoselov K. S., Geim A. K., Morozov S. V., Jiang D., Katsnelson M. I., Grigorieva I. V., Dubonos S. V. and Firsov A. A., *Nature*, **438** (2005) 197.

[5] Amanatidis I. and Evangelou S. N., *Phys. Rev. B*, **79** (2009) 205420; Libisch F., Stampfer C. and Burgdöfer J., *Phys. Rev. B*, **79** (2009) 115423; Wurm J. *et al.*, *Phys. Rev. Lett.*, **102** (2009) 056806; Huang L., Lai Y.-C., Ferry D. K., Goodnick S. M. and Akis R., *Phys. Rev. Lett.*, **103** (2009) 054101; Huang L., Lai Y.-C. and Grebogi C., *Phys. Rev. E*, **81** (2010) 055203(R); *Chaos*, **21** (2011) 013102.

[6] Blümel R. and Smilansky U., *Phys. Rev. Lett.*, **60** (1988) 477; *Physica D*, **36** (1989) 111.

[7] Doron E., Smilansky U. and Frenkel A., *Phys. Rev. Lett.*, **65** (1990) 3072.

[8] Lai Y.-C., Blümel R., Ott E. and Grebogi C., *Phys. Rev. Lett.*, **68** (1992) 3491.

[9] Bardarson J. H., Titov M. and Brouwer P. W., *Phys. Rev. Lett.*, **102** (2009) 226803.

[10] For quantum-dot systems whose classical dynamics are nonhyperbolic, it was demonstrated using semiclassical theory (Ketzmerick R., *Phys. Rev. B*, **54** (1996) 10841) and in experiments (Taylor R. P. *et al.*, *Phys. Rev. Lett.*, **78** (1997) 1952; Sachrajda A. S. *et al.*, *Phys. Rev. Lett.*, **80** (1998) 1948; Casati G., Guarneri I. and Maspero G., *Phys. Rev. Lett.*, **84** (2000) 63; Crook R. *et al.*, *Phys. Rev. Lett.*, **91** (2003) 246803) that the conductance exhibits fractal fluctuation patterns due to the hierarchical phase-space structure. An examination of the Wigner time delay and the resonance width of the conductance profile reveals that, although a power-law distribution exists for the resonance width, as in agreement with the semiclassical prediction, the energy scale is in contrast far below the mean energy level spacing [11]. It was then shown that the narrow resonances are in fact caused by the weak coupling between the localized states around the stable periodic orbits and the leads, which only couple to the chaotic part of the phase space [12,13], and the resonance line shape is well described by the Fano profile (Fano U., *Phys. Rev.*, **124** (1961) 1866). The tunneling between the chaotic part and the stable KAM island has been investigated numerically (Bäcker A., Ketzmerick R. and Monastra A. G., *Phys. Rev. Lett.* **94** (2005) 054102; Löck S., Bäcker A., Ketzmerick R. and Schlagheck P., *Phys. Rev. Lett.*, **104** (2010) 114101) and experimentally (de Moura A. P. S., Lai Y.-C., Akis R., Bird J. and Ferry D. K., *Phys. Rev. Lett.*, **88** (2002) 236804; Bäcker A. *et al.*, *Phys. Rev. Lett.*, **100** (2008) 174103).

[11] Huckestein B., Ketzmerick R. and Lewenkopf C. H., *Phys. Rev. Lett.*, **84** (2000) 5504.

[12] Weingartner B., Rotter S. and Burgdörfer J., *Phys. Rev. B*, **72** (2005) 115342.

[13] Mendoza M., Schulz P. A., Vallejos R. O. and Lewenkopf C. H., *Phys. Rev. B*, **77** (2008) 155307.

[14] Zurek W. H., *Rev. Mod. Phys.*, **75** (2003) 715.

[15] Huang L., Lai Y.-C., Ferry D. K., Goodnick S. M. and Akis R., *Phys. Rev. Lett.*, **103** (2009) 054101.

[16] Landauer R., *Philos. Mag.*, **21** (1970) 863.

[17] Datta S., *Electronic Transport in Mesoscopic Systems* (Cambridge University Press, Cambridge, UK) 1995.

[18] Rycerz A., Tworzydlo J. and Beenakker C. W. J., *EPL*, **79** (2007) 57003.

[19] Trbovic J., Minder N., Freitag F. and Schönenberger C., *Nanotechnology*, **21** (2010) 274005.

[20] Nakanishi T., Terakura K. and Ando T., *Phys. Rev. B*, **69** (2004) 115307.

[21] Kobayashi K., Aikawa H., Katsumoto S. and Iye Y., *Phys. Rev. Lett.*, **88** (2002) 256806; *Phys. Rev. B*, **68** (2003) 235304.